Supporting Information

Iron Pincer Complexes as Catalysts and Intermediates in Alkyl-Aryl Kumada Coupling Reactions

Gerald Bauer,[1] Matthew D. Wodrich,[2] Rosario Scopelliti,[1] and Xile Hu[1]*

[1] Laboratory of Inorganic Synthesis and Catalysis, [2] Laboratory for Computational Molecular Design, Institute of Chemical Sciences and Engineering, École Polytechnique Fédérale de Lausanne (EPFL), EPFL-ISIC-LSCI, BCH 3305, Lausanne, CH 1015, Switzerland.

E-mail: xile.hu@epfl.ch

Table of Content

1. Additional experimental section 4
   1.1. Syntheses: 4
      Synthesis of 2,2'-Iminodibenzoyl chloride: 4
      Synthesis of Bopa-Ph: 5
   1.2. $T_{1/2}$ – Measurements: 6
   1.3. Magnetic Bulk Susceptibility Measurements (Evan's method): 6
      [Fe(Bopa-Ph)Cl_2] (1): 7
      [Fe(Bopa-Ph)Cl$(THF)_2$] (2): 7
      [Fe(Bopa-Ph)Ph] (4): 7
      [Fe(Bopa-Ph)*o*-Tol] (5): 8
   1.4. Reaction of 4 in Presence of PhMgCl: 8
      Decomposition Experiment 8
      In-Situ formation of Mg-(Bopa)-Ph species 8
   1.5. Cross-Over Experiments: 9
   1.6. Radical trap experiments: 12
      Results Racemization Experiment: 12
      Results Ring Opening Experiment: 14
      Ring closing experiment: 14
   1.7. Attempt to prove the feasibility of the bimolecular oxidative addition mechanism: 17
      Reaction of [Fe(Bopa-Ph)Ph] (4) with *tert*-butyl-4-phenylbutaneperoxoate under UV-irradiation: 17
      Reaction of PhMgCl with *tert*-butyl-4-phenylbutaneperoxoate under UV-irradiation: 18
      Reaction of [Fe(Bopa-Ph)Ph] (4) under UV-irradiation: 19
      Reaction of *tert*-butyl-4-phenylbutaneperoxoate under UV-irradiation: 21
   1.8. Kinetic studies: 22
      Dependence on PhMgCl: 23
      Dependence on [Fe(Bopa-Ph)Cl$(THF)_2$] (2): 26
      Dependence on (3-iodobutyl)benzene: 28
      Confirmation of the 0^{th}-order by integrated rate law: 30
   1.9. Determination of the Resting State: 32
2. Crystal Structures 34
   2.1. [Fe(Bopa-Ph)Cl_2] (1): CCDC number 1004323 34
   2.2. [Fe(Bopa-Ph)Cl$(THF)_2$] (2): CCDC number 1004324 34
   2.3. [Fe(Bopa-Ph)*o*Tol] (5): CCDC number 1004325 35

3. Computational Details 36
4. Appendix 39
5. References 43

1. Additional experimental section

1.1. Syntheses:

Synthesis of 2,2'-Iminodibenzoyl chloride:

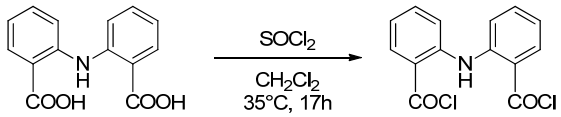

2,2'-Iminodibenzoic acid (21.0 g, 1,0 equiv.) was suspended in 100 mL CH_2Cl_2 and thionyl chloride (18.0 mL, 3.0 equiv.) was added. The suspension was heated to reflux overnight. The formed yellow solid was filtered off and washed twice with 20 mL cold CH_2Cl_2. The filtrate was carefully extracted with water to quench the reaction. The organic phase was dried over Na_2SO_4 and evaporated to dryness. The crude product (from the filtrate) was recrystallized from CH_2Cl_2 and hexane. The obtained solids were combined.

Yield: 21.8 g (91%), bright yellow solid

^{1}H NMR (400 MHz, $CDCl_3$): δ 10.36 (s, 1H), 8.27 (d, J=8.5 Hz, 2H), 7.54 - 7.49 (m, 4H), 7.07 (ddd, J=7.1, 2.4 Hz, 2H).

^{13}C {1H} NMR (101 MHz, $CDCl_3$) δ 168.45, 144.04, 135.91, 135.72, 121.71, 121.04, 118.73.

Elemental analysis calculated (%) for $C_{14}H_9Cl_2NO_2$: C 57.17, H 3.08, N 4.76; found: C 57.05, H 3.04, N 4.60

Melting Point: 163 – 165°C

Synthesis of Bopa-Ph:

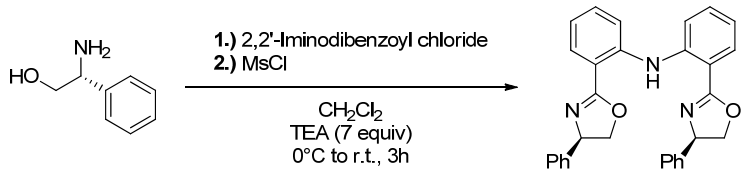

The procedure is based on the literature procedure by Lu S.-F. et al.[8]

R-(-)-Phenylglycinol (4.1 g, 2.0 equiv) was dissolved in 150 mL CH_2Cl_2 and triethylamine (14.5 mL, 7.0 equiv; freshly distilled from KOH!) was added. The solution was cooled to 0°C and 2,2'-iminodibenzoyl chloride (4.4 g, 1.0 equiv) was added slowly. After addition the cooling bath was removed and the solution stirred for 1h at room temperature (r.t.). The conversion was checked by TLC. The solution was cooled again to 0°C and methanesulfonyl chloride (MsCl) was slowly added. The reaction mixture was warmed to r.t. and stirred for 2h. The conversion was checked by TLC.

The reaction mixture was quenched with water and the organic phase was extracted with water, saturated sodium bicarbonate solution and dried over Na_2SO_4. The crude product (99%) was purified by column chromatography (EtOAc:Hexane: 1:9).

Yield: 4.9 g (71%), yellowish white solid

^{1}H NMR (400 MHz, $CDCl_3$): δ 11.10 (s, 1H), 7.91 (dd, *J* = 7.9, 1.6 Hz, 2H), 7.60 – 7.53 (m, 2H), 7.40 – 7.32 (m, 2H), 7.28 – 7.13 (m, 10H), 7.00 – 6.91 (m, 2H), 5.20 (dd, *J* = 10.0, 8.2 Hz, 2H), 4.50 (dd, *J* = 10.1, 8.3 Hz, 2H), 4.02 (t, *J* = 8.2 Hz, 2H).

^{13}C {^{1}H} NMR (101 MHz, $CDCl_3$): δ 164.31, 143.28, 142.74, 131.64, 130.74, 128.64, 127.42, 126.81, 119.99, 118.26, 115.89, 73.86, 70.16.

1.2. $T_{1/2}$ – Measurements:

Stock solutions with (3-iodobutyl)benzene (0.250M, **Sol.A**) and naphthalene as an internal standard, [Fe(Bopa-Ph)Ph] (6.44mM, **Sol.B**), PhMgCl in THF (12.5mM, **Sol.C**), and PhLi in n-Bu_2O (12.5mM; stock solution in THF, **Sol.D**).

Standard experiment:

1.0 mL of **Sol.B** was put in a vial and cooled to -40°C under stirring. 0.5 mL of **Sol.A** was added and 50 µL samples were taken after 0.5, 1, 2, 4, 8, 12, 16, 30, 60 minutes and immediately quenched with 100 µL 2-propanol. The yield was determined by GC (a FI-Detector was used for quantification).

Experiment with additives:

1.0 mL of **Sol.B** was put in a vial and cooled to -40°C and 0.5 mL of **Sol.A** was added. Immediately after 0.5 mL of either **Sol.C**, or **Sol.D**, was added. 50 µL samples were taken after 15, 30, 45, and 60 seconds, and immediately quenched with 100 µL 2-propanol. The yield was determined by GC (a FI-Detector was used for quantification).

1.3. Magnetic Bulk Susceptibility Measurements (Evan's method):

The sample is weight into a J.Young-NMR tube and dissolved in a – preferably – non-coordinating solvent. TMS was added as an internal standard (homogeneous phase). Afterwards a capillary with exactly the same solvent and standard was inserted into the NMR tube (heterogeneous phase). Meanwhile the NMR probe was heated to around 25°C (the exact temperature was measured) and the sample was inserted. After about 5 minutes (when the temperature was constant) a spectrum was measured. The susceptibility is calculated by the following formula:

$$\mu_{eff} = 2.828\sqrt{\frac{\Delta_x T}{4\pi c S 10^3}} \quad \text{(Eq. 1)}$$

μ_{eff}	Effective magnetic moment [μ_b]
Δ_x	Bulk magnetic susceptibility shifts [ppm]
T	Temperature [K]
c	Concentration [mol*L^{-1}]
S	Spherical factor (1/3 for a cylindrical shaped sphere parallel to the magnetic field)

The number of unpaired electrons can be approximated by spin-only formula, which is direct proportional to the magnetic moment (μ_{eff}):

$$\mu_{eff} = \sqrt{n(n+2)} \quad \text{(Eq. 2)}$$

n	number of unpaired electrons

[Fe(Bopa-Ph)Cl_2] (1):

m(**1**)	12.3 mg
m(C_6D_6)	488.4 mg
Standard	TMS
T [K]	297.65
Δ_x [ppm]	0.43
μ_{eff}	5.61 µb

[Fe(Bopa-Ph)Cl(THF)$_2$] (2):

m(**2**)	4.8 mg
m(THF-d_8)	487.0 mg
Standard	TMS
T [K]	308.95
Δx [ppm]	0.62
μ_{eff}	5.11 µb

[Fe(Bopa-Ph)Ph] (4):

m(**4**)	7.0 mg
m(C_6D_6)	420.1 mg
Standard	TMS

T [K]	299.55
Δ_x [ppm]	1.17
μ_{eff}	5.00 µb

[Fe(Bopa-Ph)*o*-Tol] (5):

m(**5**)	32.6 mg
m(C_6D_6)	519.8 mg
Standard	TMS
T [K]	302.15
Δ_x [ppm]	3.88
μ_{eff}	4.76 µb

1.4. Reaction of 4 in Presence of PhMgCl:

Decomposition Experiment

15.3 mg (25.9 µmol) of 4 was dissolved in 0.5 mmol d8-THF and 14 µL (26.0 µmol, 1.0 equiv.) PhMgCl in THF (1.86 M) and a drop of TMS were added via a Hamilton syringe. The sample was transferred to an NMR tube, and the spectra were measured in regular intervals (Figure S1). During the measurement one could see that the log signal was strongly shifting.

In-Situ formation of Mg-(Bopa)-Ph species

9.3 mg (20.2 µmol) of Bopa-Ph was dissolved in 0.5 mL d8-THF, and its 1H-NMR was recorded. Then 20 µL (37.2 µmol, 1.8 equiv.) of PhMgCl in THF (1.86 M) was e added. The solution turned immediately fluorescent yellow. A 1H-NMR spectrum was recorded (Figure S1).

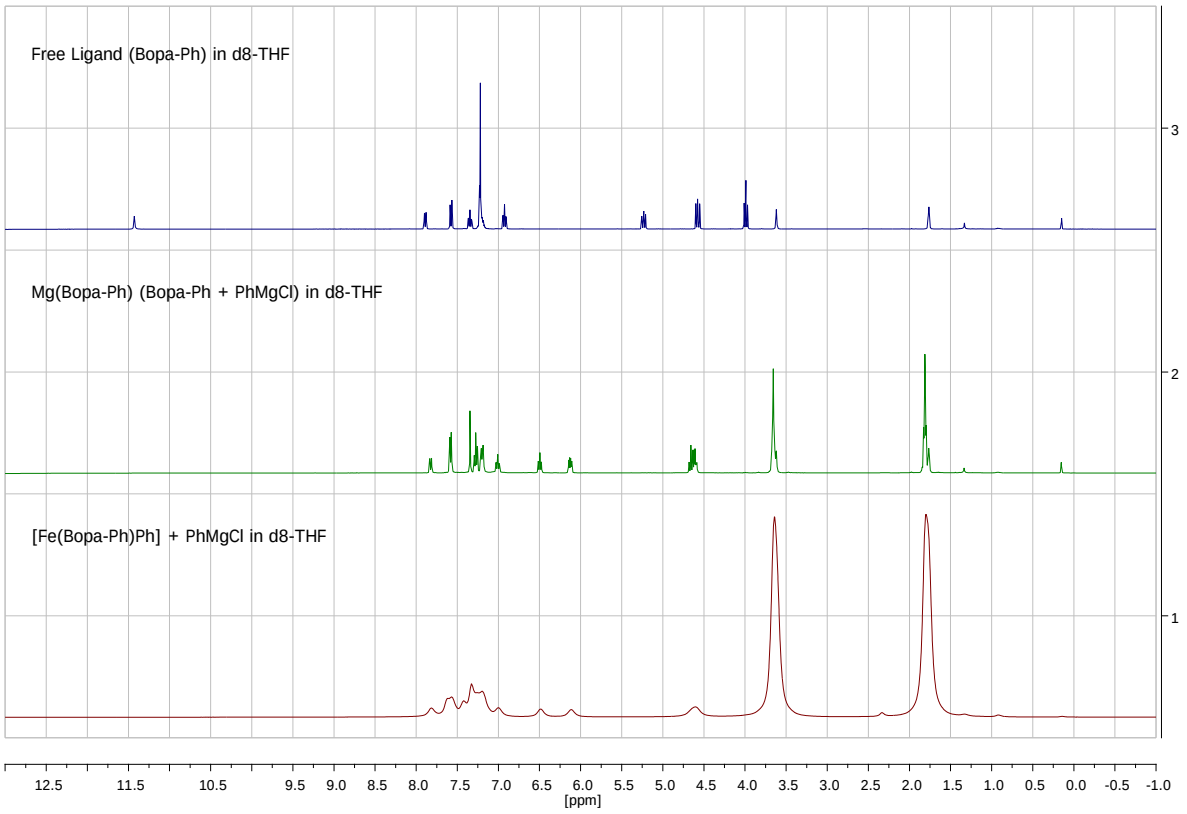

Figure S1. Comparison of the spectra of the free Bopa-Ph, Mg(Bopa-Ph), and the mixture of of **4** with one equivalent PhMgCl.

1.5. Cross-Over Experiments:

General remarks:

Two experiments were conducted (see scheme below).

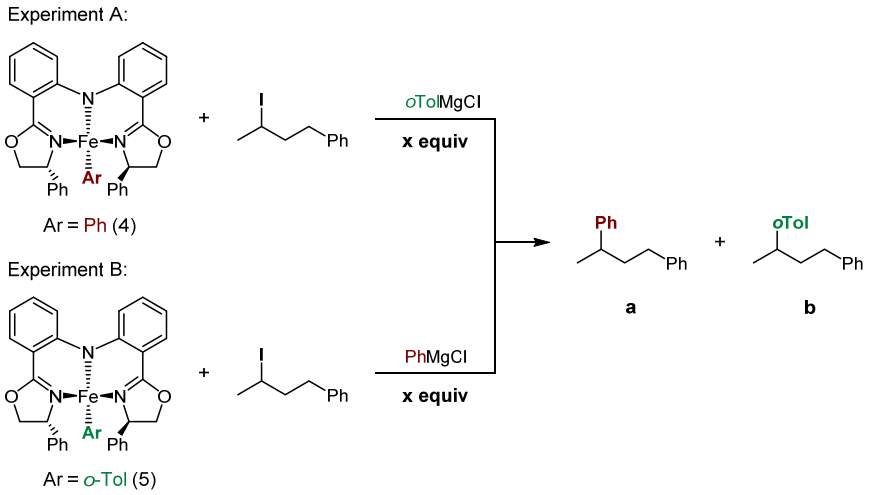

Before the following standard solutions were prepared:

Sol.A: (3-Iodobutyl)benzene (11.9 mg, 47.5 µmol), and naphthalene (4.6 mg, 35.9 µmol) as an internal standard were dissolved in 5.0 mL THF

Sol.B: [Fe(Bopa-Ph)Ph] (15.0 mg, 25.4 µmol) were dissolved in 5.0 mL THF

Sol.C: *o*-TolMgCl in THF (0.68 M, 0.33 mL) were dissolved in 25.0 mL THF

Sol.D: [Fe(Bopa-Ph) *o*-Tol] (15.6 mg, 25.8 µmol) were dissolved in 5.0 mL THF

Sol.E: PhMgCl in THF (1.86 M, 0.12 mL) were dissolved in 25.0 mL THF

The solutions were mixed as followed (Table S1):

Table S1. Sample composition of the results corresponding to Figure S2 (left graph).

	Experiment A			Experiment B		
	Sol.A	Sol.B	Sol.C	Sol.A	Sol.D	Sol.E
A	0.5 mL	1.0 mL	0.5 mL	0.5 mL	1.0 mL	0.5 mL
B	0.5 mL	1.0 mL	0.4 mL	0.5 mL	1.0 mL	0.4 mL
C	0.5 mL	1.0 mL	0.3 mL	0.5 mL	1.0 mL	0.3 mL
D	0.5 mL	1.0 mL	0.2 mL	0.5 mL	1.0 mL	0.2 mL

The complex stock solution (**Sol.B** or **Sol.D**) were put in a vial and **Sol.A** was added. Immediately after the Grignard stock solution (**Sol.C** or **Sol.E**) was added. And the reaction was allowed to stir for an additional 30 min at room temperature. The reaction was quenched by adding 100 µL of ethanol. The coupling products were determined by GC/MS using a FI-detector for quantification.

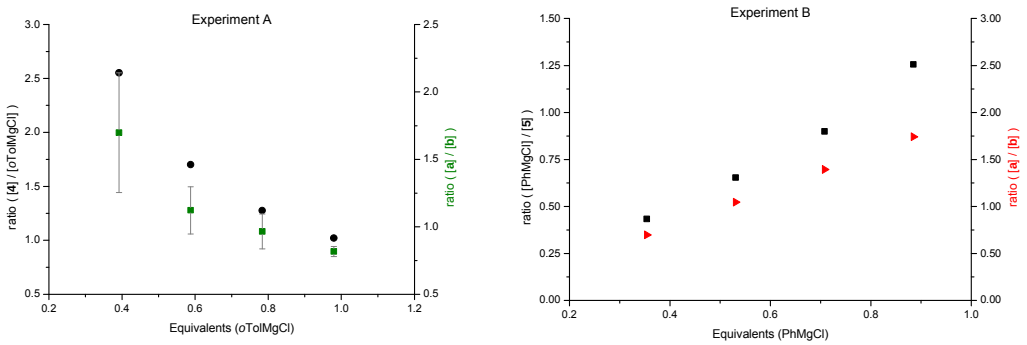

Figure S2. Left Graph: Experiment A was repeated twice with **4** and *o*TolMgCl in order to prove the reproducibility. It shows the Ph/*o*Tol ratio of the starting materials (black dots) in comparison to Ph/*o*Tol ratio of the products (green rectangles); this graph corresponds to Table 2 – see main text. Right Graph: Experiment B was only conducted once. It shows the Ph/*o*Tol ratio of both starting material (black rectangles) and product (red triangle).

1.6. Radical trap experiments:

General procedure:

The bromoalkane (0.25 mmol) and **1** (12.5 μmol) were weighed into a vial and dissolved in THF (2.0 mL). PhMgCl in THF (0.30 mmol) were added dropwise over a time period of 5 minutes at room temperature. After addition the solution stirred for another 10 minutes. The solution was quenched with water and further acidified with HCl (1M) and extracted with 3 x 20 mL of CH_2Cl_2. The combined organic phases were dried over Na_2SO_4 and the solvent was evaporated to dryness.

Results Racemization Experiment:

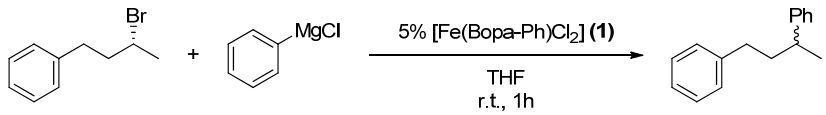

The sample was purified before the HPLC run by preparative TLC (solvent: hexane).

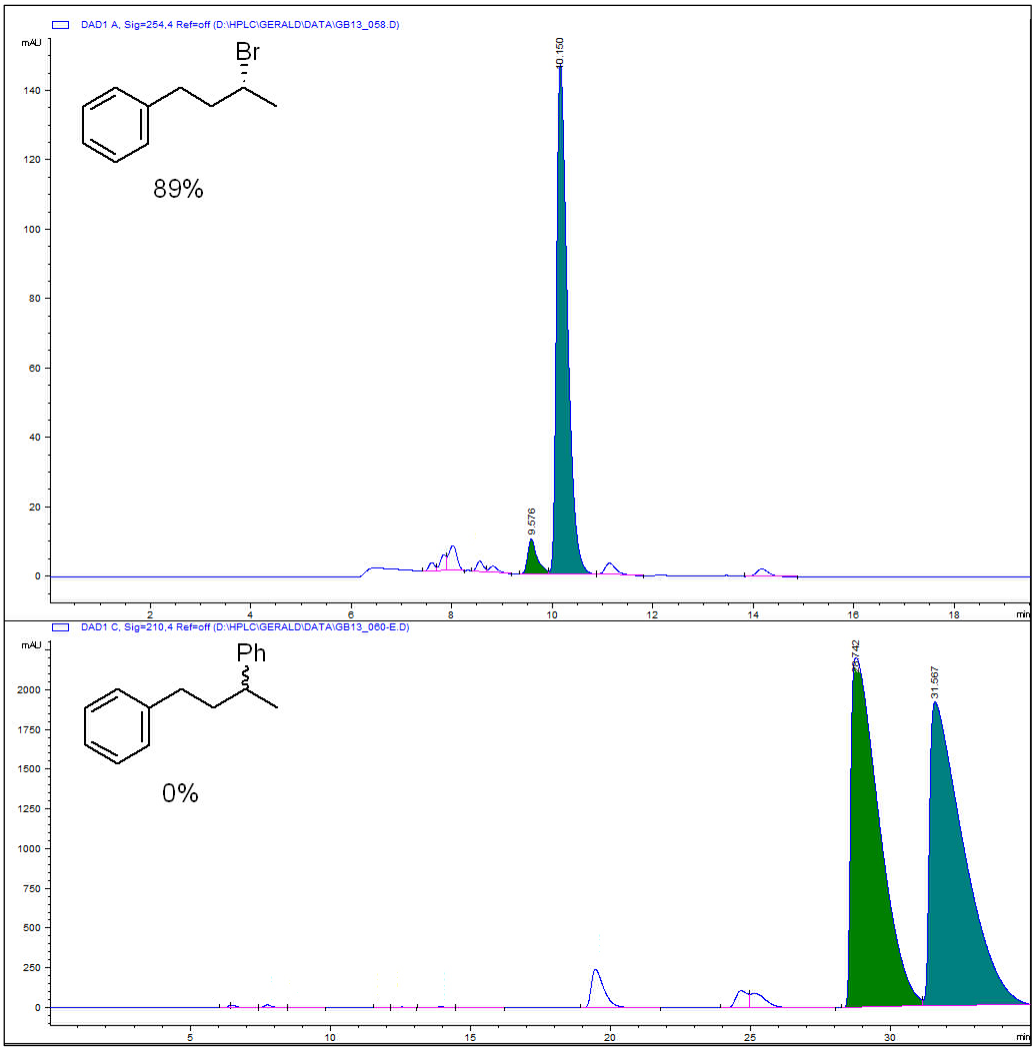

Figure S3. HPLC spectra of R-(3-bromobutyl)benzene and 1,3-diphenylbutane to show the racemization during the cross coupling reaction.

Results Ring Opening Experiment:

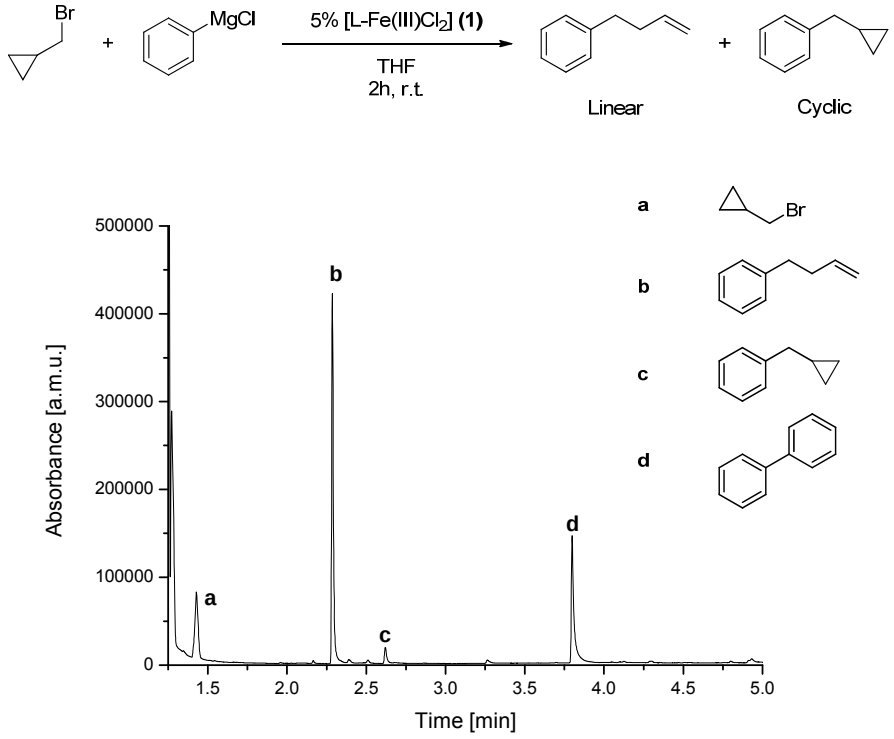

Figure S4. GC spectrum of the products formed during the cross-coupling of (bromomethyl)cyclopropane with PhMgCl.

It was attempted to isolate the product from the crude mixture by preparative TLC (mobile phase: hexanes). But it was co-isolated with the byproducts. The coupling product (**b**) was thus identified by ^{1}H-NMR spectroscopy by comparing with the commercially available 4-phenyl-1-butene (Figure S19).**Ring closing experiment:**

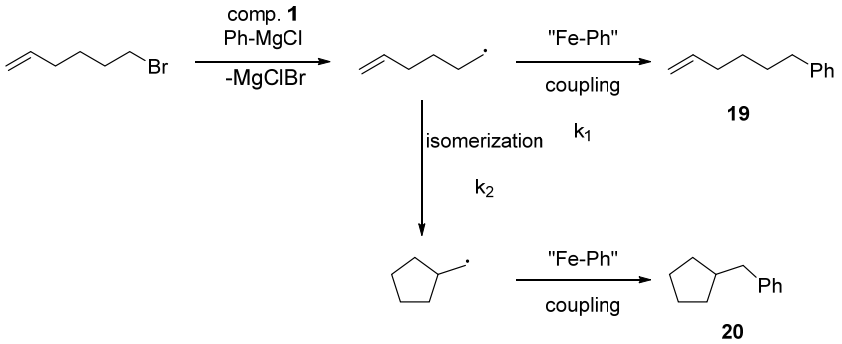

General remark:

In one experiment 4 samples were prepared with variable catalyst loadings. The reaction and work-up procedure is described in the above section "General Procedure" (reaction was performed at room temperature overnight). Two consecutive experiments were performed. Beforehand two standard solutions were prepared:

Sol.A: [Fe(Bopa-Ph)Cl_2] (73.2 mg, 125.1 µmol) were dissolved in 5.0 mL THF (c = 25.0mM)

Sol.B: 6-Bromo-1-hexene (408.6 mg, 2.51 mmol) and dodecane as an internal standard (218.5 mg, 1.28 mmol) were dissolved in 10.0 mL THF (c = 251 mM)

The solutions were mixed according to Table S2:

Table S2. Sample composition of a single experiment.

Sample	V (Sol.A)	V (THF)	V (Sol.B)	Catalyst loading [%]
A	1.0 mL	0.0 mL	1.0 mL	10%
B	0.7 mL	0.3 mL	1.0 mL	7%
C	0.3 mL	0.7 mL	1.0 mL	3%
D	0.1 mL	0.9 mL	1.0 mL	1%

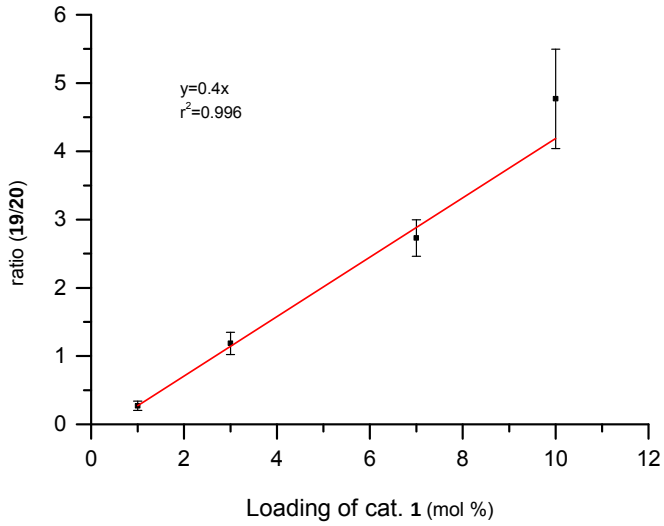

Figure S5. Dependence of the ratio of compounds **19**/**20** relative to the catalyst loading.

Identification:

The formed products were separated and identified by GC/MS. The yields were determined using naphthalene as an internal standard and a FI-detector for quantification. Further on, the crude mixture was purified by column chromatography (gradient 1% ethyl acetate to 3% in hexane). The linear products (**b**, **c**) were isolated (sample consisted of biphenyl impurities) and identified by ^{1}H-NMR and compared to the literature.[9]

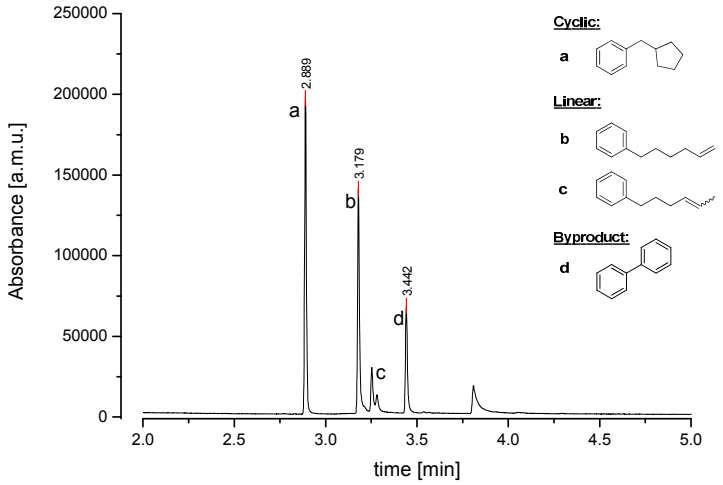

Figure S6. GC spectrum of the products formed during the cross-coupling of 6-bromo-1-hexene with PhMgCl.

NMR is shown in Figure S20 (appendix).

^{1}H NMR (400 MHz, $CDCl_3$) δ 7.35 – 7.23 (m, 5H), 5.92 – 5.82 (m, 1H), 5.08 – 4.99 (m, 2H), 2.67 (t, J = 7.6 Hz, 2H), 2.15 – 2.11 (m, 2H), 1.76 – 1.64 (m, 2H), 1.52 – 1.46 (m, 2H).

1.7. Attempt to prove the feasibility of the bimolecular oxidative addition mechanism:

Reaction of [Fe(Bopa-Ph)Ph] (4) with *tert*-butyl-4-phenylbutaneperoxoate under UV-irradiation:

A solution with [Fe(Bopa-Ph)Ph] (6.44mM, 1.0 mL) and dodecane as an internal standard was put in a J. Young-NMR tube and *tert*-butyl-4-phenylbutaneperoxoate (5.6mg; 23.7 µmol) was added. The sample was put in a Rayonet Photochemical reactor for 1.5h. The reaction mixture was quenched with methanol and the coupling products were checked by GC/MS using dodecane as an internal standard (a FI-detector was used for quantification). The 1,3-diphenylpropane was independently synthesized from 1-bromo-3-phenylpropane using the protocol in chapter 3.2. The product was confirmed by GC/MS and ^{1}H-NMR (Figures S21 – 23). The other peaks shown in Figure S7 were found in the blank reaction and therefore not taken under consideration. The yields for the phenyl containing products which is derived from [Fe(Bopa-Ph)Ph] were calculated to be 20% for compound (a) and 27% for compound (b) (Figure S7).

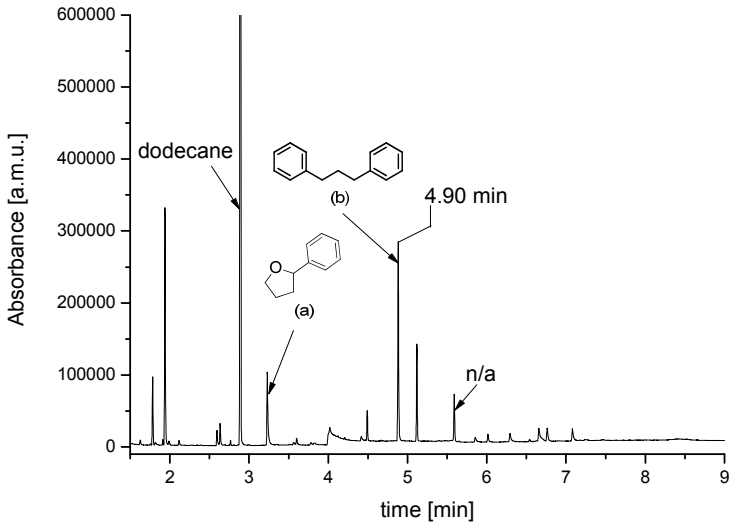

Figure S7. GC spectrum of the products formed during the UV irradiation of **4** in presence of *tert*-butyl-4-phenylbutaneperoxoate. The other peaks came from the background reaction (Figure S25) and were not further taken under consideration.

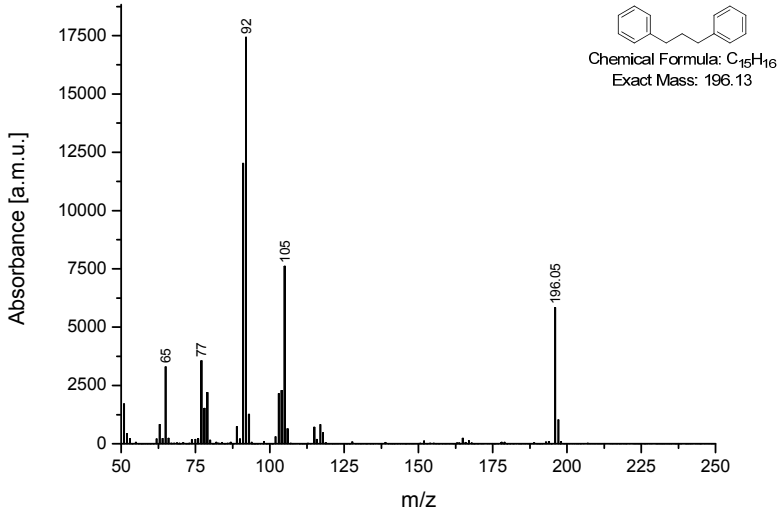

Figure S8. Averaged MS-spectrum taken from the crude GC spectrum between 4.88 – 4.89 min retention time.

Reaction of PhMgCl with *tert*-butyl-4-phenylbutaneperoxoate under UV-irradiation:

A J. Young-NMR tube was charged with 1.0 mL THF and PhMgCl in THF (20 µL, 1.90 M, 38.0 µmol), and *tert*-butyl-4-phenylbutaneperoxoate (6.8 mg, 28.8 µmol) were added. The sample was put in a Rayonet Photochemical reactor and irradiated for 1.5h. The reaction mixture was put in a GC vial and analyzed by GC/MS. No starting material could be found meaning that all the *tert*-butyl-4-phenylbutaneperoxoate was reacted. The resulting spectrum (Figure S9) shows no formation of 1,3-diphenylpropane (coupling product of the phenylpropyl radical with PhMgCl).

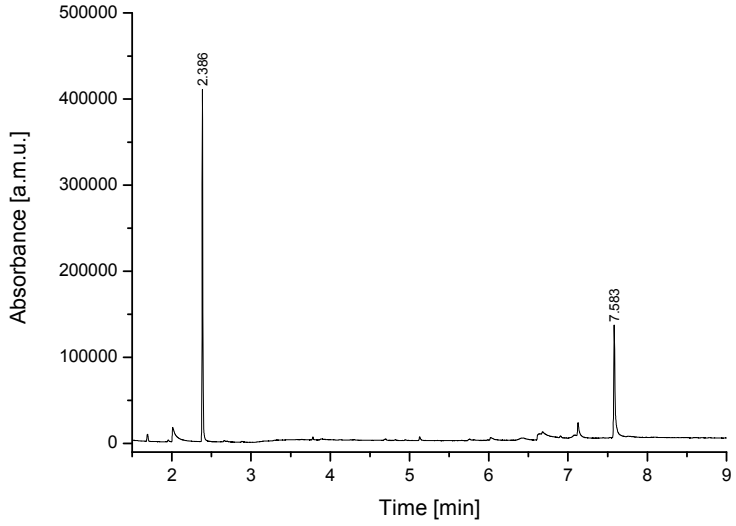

Figure S9. GC spectrum of the products of blank reaction of PhMgCl and *tert*-butyl-4-phenylbutaneperoxoate under UV irradiation. Neither of the formed products were observed in the reaction of *tert*-butyl-4-phenylbutaneperoxate with **4**.

Reaction of [Fe(Bopa-Ph)Ph] (4) under UV-irradiation:

A J. Young-NMR tube was charged with 0.5 mL THF-d_8 and [Fe(Bopa-Ph)Ph] (1.9 mg, 3.2 μmol) was added. The NMR tube was placed in the NMR spectrometer and a ^{1}H-NMR spectrum was recorded. Afterwards the sample was put in a Rayonet Photochemical reactor and irradiated for 1.5h. After the irradiation the sample was measured again. The NMR showed that no complex decomposed during the irradiation (Figure S11).

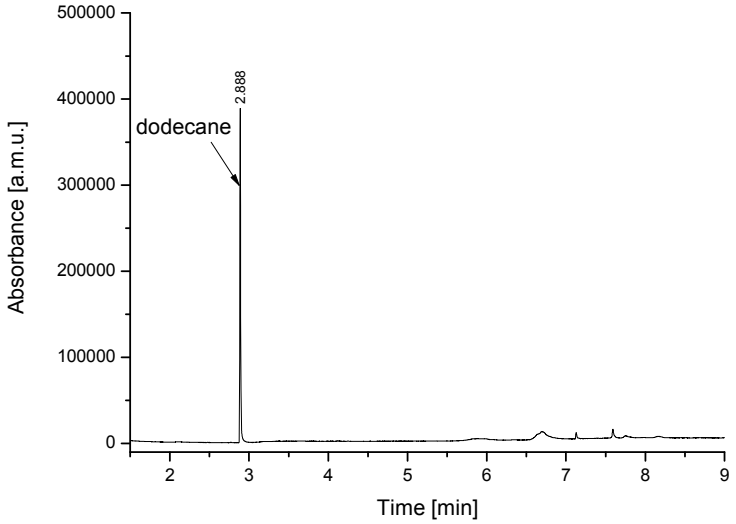

Figure S10. GC spectrum of the products of blank reaction of **4** in THF under UV irradiation.

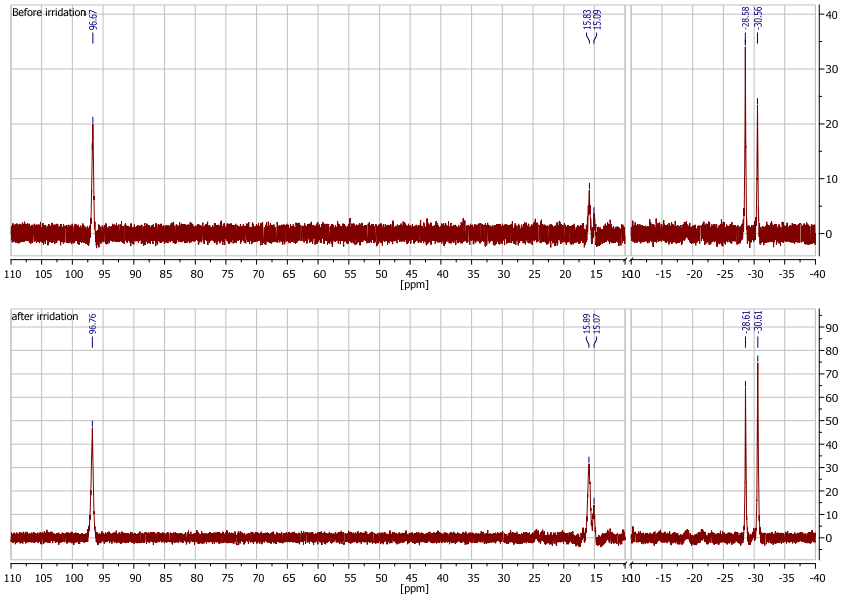

Figure S11. NMR spectra of [Fe(Bopa-Ph)Ph] (**4**) before and after the irradiation with UV light (out of clarity reasons the residue solvent signals in the range from -10 - 10 ppm were omitted).

Reaction of *tert*-butyl-4-phenylbutaneperoxoate under UV-irradiation:

A J. Young-NMR tube was charged with 1.0 mL THF and *tert*-butyl-4-phenylbutaneperoxoate (12.2 mg, 51.6 µmol) was added. The sample was put in a Rayonet Photochemical reactor and irradiated for 1.5h. The reaction mixture was put in a GC vial and analyzed by GC/MS. No starting material could be found meaning that all the *tert*-butyl-4-phenylbutaneperoxoate reacted. The resulting spectrum (Figure S12) shows the formed products.

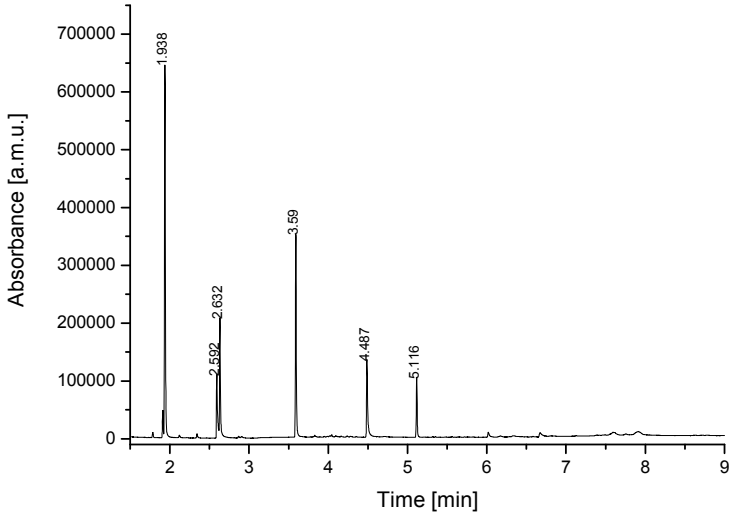

Figure S12. GC spectrum of the products of blank test of *tert*-butyl-4-phenylbutaneperoxate in THF under UV irradiation.

1.8. Kinetic studies:

General considerations:

The reaction rate *v* can be calculated as followed:

$$v = k[Complex]^a[Alkyl]^b[PhMgCl]^c \quad \text{(Eq. 3)}$$

If the concentration of one reaction partner is varied while the other one are kept constant, one can simplify equation 3 to:

$$v = k_{eff}[X]^n \quad \text{(Eq. 4)}$$

This assumption can be drawn in the first few per cent of the formed product (≤ 10%). Since the other reactants are in large excess than the formed product, they can be considered as constant. Further logarithmic calculus gives a linear dependence of rate and concentration:

$$\ln(v) = \ln(k_{eff}) + n * ln([X]) \quad \text{(Eq. 5)}$$

The reaction rate *n* can then be determined by plotting ln(*v*) versus ln([X]). The slope then gives the order *n* of the reaction.

General remarks:

In the first screening reactions to find the ideal concentration and temperature range, it was noticed that the reaction rate of the reduction from [Fe(Bopa-Ph)Cl_2] to [Fe(Bopa-Ph)Cl$(THF)_2$] drastically reduces at lower temperatures. Since there was no noticeable reaction at -84°C (melting point of ethyl acetate) we decided to perform the kinetic measurements with [Fe(Bopa-Ph)Cl$(THF)_2$].

Dependence on PhMgCl:

General remarks:

In one experiment 8 reaction solutions were prepared with variable Grignard concentrations. The reactions were performed in a consecutive order to maintain the same reaction and sampling conditions. For each reaction 10 GC samples were prepared. To achieve a constant reaction temperature a slurry of melting ethyl acetate (m.p. = -84°C) was prepared before the experiment. The example given below depicts one single experiment. In order to determine the order of the reaction the mean value of at least three independent experiments was taken.

Before the experiment three stock solutions were prepared:

Sol.A: 1.0 mL of PhMgCl in THF (1.85 M) were diluted to 5.0 mL THF solution (c = 0.37 M).

Sol.B: (3-Iodobutyl)benzene (289.6 mg, 1.11 mmol) and naphthalene (60.3 mg, 0.47 mmol) as an internal standard were diluted to 9.0 mL THF solution (c = 0.124 M).

Sol.C: [Fe(Bopa-Ph)Cl$(THF)_2$] (43.8 mg, 63.1 μmol) were dissolved in 5.0 mL THF (c = 12.6 mM).

Inside the glove box screw vials with a stirring bar were filled with 0.2, 0.3, 0.4, 0.5, 0.6, 0.7, 0.8, and 1.0 mL of **Sol.A**, then 1.0 mL of **Sol.B** was added. The vials were filled up with THF to a total volume of 2.0 mL. The vials were closed with a rubber septum. 0.5 mL of **Sol.C** was put in 1.0 mL insulin syringes (the tip of the needle was put in a rubber stopper to minimize the exposure to air). The vials were taken out of the glove box and attached to the Schlenk line by piercing a needle through the septum. The following procedure was done consecutively with every reaction vial: The vial was put in the ethyl acetate slurry, and stirred for about 5 minutes (to be sure that the temperature is constant). Then the rubber septum was

removed from the vial (while maintaining the nitrogen flow). **Sol.C** was added at once. An aliquot of 100 μL was taken in regular intervals (depending on the concentration of Grignard reagent, and hence its reaction rate) and immediately pipetted in a GC vial containing 50 μL acetonitrile. The GC vials were then filled with diethyl ether and analyzed by GC (a FI-detector was used for quantification).

The yields of the 1,3-diphenylbutane were determined in respect to naphthalene as an internal standard. Figure S13 shows the results (yield versus time) of a single experiment. In order to determine the reaction rate, the data points (up to 10% yield) were fitted linear. The reaction rates were then logarithmized, averaged and then plotted versus the logarithm of the PhMgCl concentration (Graph A, Figure 5).

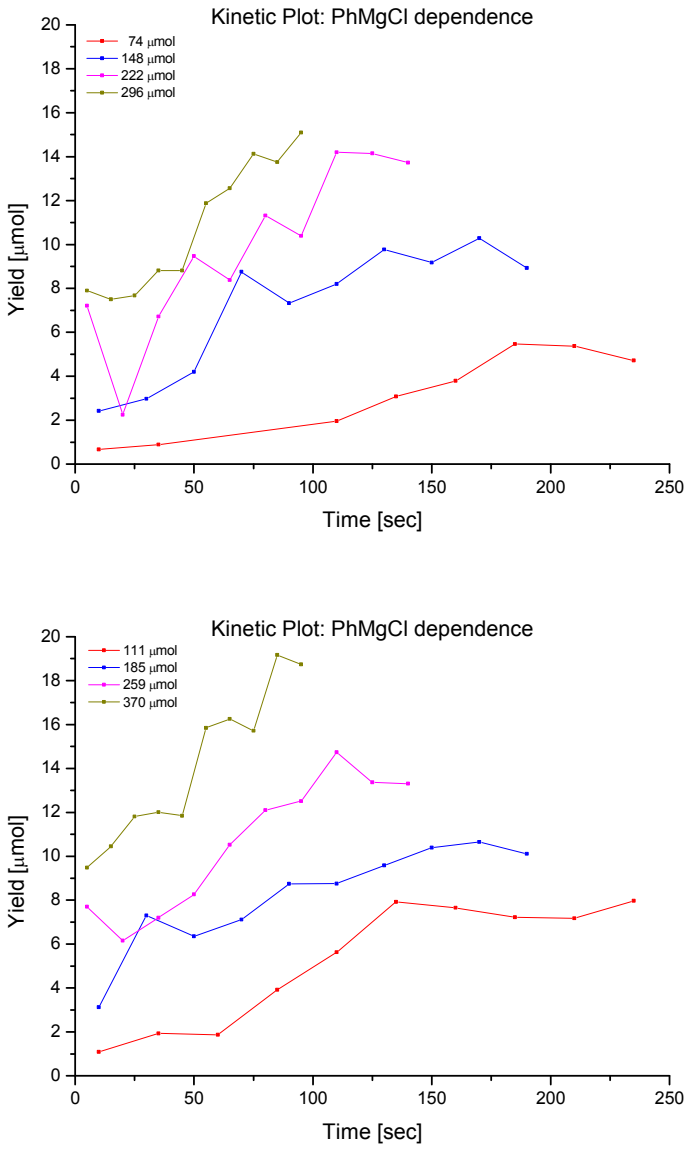

Figure S13. Reaction profile of single experiments under variable concentrations of PhMgCl.

Dependence on [Fe(Bopa-Ph)Cl(THF)$_2$] (2):

General remarks:

The results depicted in Graph B (Figure 5) consist of two sets of experiments with each 4 reactions. The first set covers a catalyst loading of 4.0, 5.0, 6.0, and 7.0%, and the second set covers a catalyst loading of 1.8, 3.6, 5.4, 7.2%. In each set different solutions with variable complex concentrations were prepared. The reactions were performed in a consecutive order to maintain the same reaction and sampling conditions. For each reaction 10 GC samples were prepared. To achieve a constant reaction temperature a slurry of melting ethyl acetate (m.p. = -84°C) was prepared before the experiment. The example given below depicts one single experiment. In order to determine the order of the reaction the mean value of three independent experiments (in each set) was taken.

Before the experiment three stock solutions were prepared:

Sol.A: [Fe(Bopa-Ph)Cl(THF)$_2$] (38.9 mg, 56.0 μmol) were dissolved in 5.0 mL THF (c = 11.2 mM).

Sol.B: (3-Iodobutyl)benzene (290.9 mg, 1.12 mmol) and naphthalene (75.6 mg, 0.59 mmol) as an internal standard were diluted to 9.0 mL THF solution (c = 0.124 M).

Sol.C: 0.95 mL of PhMgCl in THF (1.85 M) were diluted to 7.0 mL THF solution (c = 0.25 M).

Inside the glove box screw vials with a stirring bar were filled with 0.2, 0.4, 0.6, and 0.8 mL of **Sol.A**, then 1.0 mL of **Sol.B** was added. The vials were filled up with THF to a total volume of 2.0 mL. The vials were closed with a rubber septum. 0.5 mL of **Sol.C** was put in 1.0 mL insulin syringes (the tip of the needle was put in a rubber stopper to minimize the exposure to air). The vials were taken out of the glove box and attached to the Schlenk line by

piercing a needle through the septum. The following procedure was done consecutively with every reaction vial: The vial was put in the ethyl acetate slurry, and stirred for about 5 minutes (to be sure that the temperature is constant). Then the rubber septum was removed from the vial (while maintaining the nitrogen flow). **Sol.C** was added at once. An aliquot of 100 µL was taken in regular intervals (depending on the complex concentration, and hence its reaction rate) and immediately pipetted in a GC vial containing 50 µL acetonitrile. The GC vials were then filled with diethyl ether and analyzed by GC (a FI-detector was used for quantification).

The yields of the 1,3-diphenylbutane were determined using naphthalene as an internal standard. Figure S14 shows the results (yield versus time) of a single experiment. In order to determine the reaction rate, the data points (up to 10% yield) were fitted linear. The reaction rates were then logaritmized, averaged and then plotted versus the logarithm of [Fe(Bopa-Ph)Cl(THF)$_2$] concentration (Graph B, Figure 5).

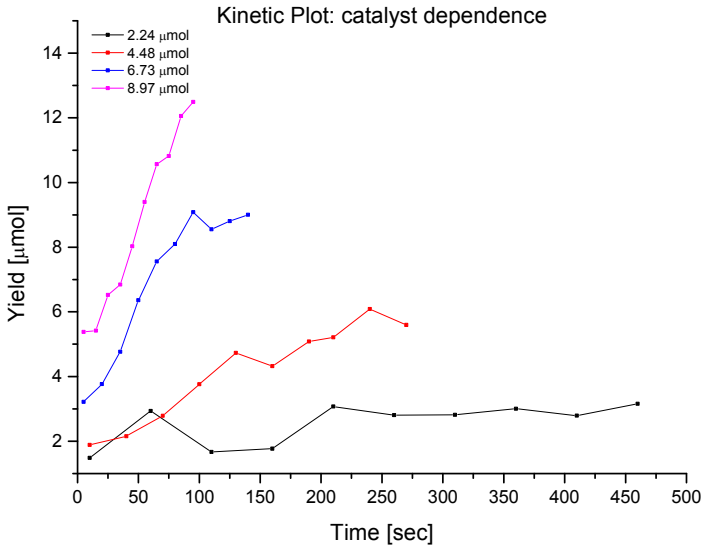

Figure S14. Reaction profile of a single experiment under variable concentrations of **2**.

Dependence on (3-iodobutyl)benzene:

General remarks:

In one experiment 6 reaction solutions were prepared with variable substrate concentrations. The reactions were performed in a consecutive order to maintain the same reaction and sampling conditions. For each reaction 10 GC samples were prepared. To achieve a constant reaction temperature a slurry of melting ethyl acetate (m.p. = -84°C) was prepared before the experiment. The example given below depicts one single experiment. In order to determine the order of the reaction the mean value of at eight independent experiments was taken.

Before the experiment three stock solutions were prepared:

Sol.A: (3-Iodobutyl)benzene (244.2 mg, 0.94 mmol) and naphthalene (62.7 mg, 0.49 mmol) as an internal standard were diluted to 5.0 mL THF solution (c = 0.188 M).

Sol.B: [Fe(Bopa-Ph)Cl(THF)$_2$] (30.7 mg, 44.2 μmol) were dissolved in 7.0 mL THF (c = 6.3 mM).

Sol.C: 0.54 mL of PhMgCl in THF (1.85 M) were diluted to 4.0 mL THF solution (c = 0.25 M).

Inside the glove box screw vials with a stirring bar were filled with 0.5, 0.6, 0.7, 0.8, 0.9, and 1.0 mL of **Sol.A**, then 1.0 mL of **Sol.B** was added. The vials were filled up with THF to a total volume of 2.5 mL. The vials were closed with a rubber septum. 0.5 mL of **Sol.C** was filled in 1.0 mL syringes (the tip of the needle was put in a rubber stopper to minimize the exposure to air). The vials were taken out of the glove box and attached to the Schlenk line by piercing a needle through the septum. The following procedure was done consecutively with every reaction vial: The vial was put in the previously prepared ethyl acetate slurry, and stirred for about 5 minutes (to be sure that the temperature is constant). Then the rubber

septum was removed from the vial (while maintaining the nitrogen flow). **Sol.C** was added at once. An aliquot of 100 µL was taken every 20 seconds and immediately pipetted in a GC vial containing 50 µL acetonitrile. The GC vials were then filled with diethyl ether and analyzed by GC (a FI-detector was used for quantification).

The yields of the 1,3-diphenylbutane were determined in respect to naphthalene as an internal standard. Figure S15 shows the results (yield versus time) of a single experiment. In order to determine the reaction rate, the data points (up to 10% yield) were fitted linear. The reaction rates were then logaritmized, averaged and then plotted versus the logarithm of (3-iodobutyl)benzene concentration (Graph C, Figure 5).

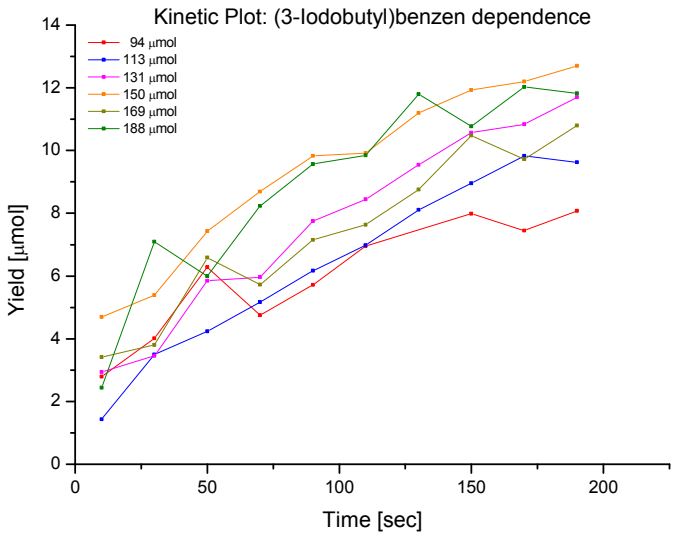

Figure S15. Reaction profile of a single experiment under variable concentrations of (3-iodobutyl)benzene.

Confirmation of the 0th-order by integrated rate law:

General considerations:

The reaction rate *v* can be calculated as followed (with the previously shown 2nd order for catalyst loading and 1st order for Grignard loading):

$$v = \frac{d[Alkyl]}{dt} = -k[Complex]^2[PhMgCl]^1[Alkyl]^n \quad \text{(Eq. 6)}$$

In a reaction where A + B → C without any side reaction the [A] = [B] at any time of the reaction. Furthermore, the concentration of the catalyst stays constant throughout the reaction. Hence equation 6 can be simplified to:

$$\frac{d[Alkyl]}{dt} = -k_{eff} * [Alkyl]^1 * [Alkyl]^n = -k_{eff} * [Alkyl]^{(1+n)} \quad \text{(Eq. 7)}$$

With:

$$k_{eff} = k * [Complex]^2 \quad \text{(Eq. 8)}$$

Therefore:

$$\int_{[Alkyl]_0}^{[Alkyl]} \frac{1}{[Alkyl]^{(1+n)}} d[Alkyl] = -k_{eff} \int_{t_0}^{t} dt \quad \text{(Eq. 9)}$$

In case:

n = 0: $$\ln(\frac{[Alkyl]}{[Alkyl]_0}) = -k_{eff} * t \quad \text{(Eq. 10)}$$

n = 1: $$\frac{[Alkyl]_0 - [Alkyl]}{[Alkyl][Alkyl]_0} = k_{eff} * t \quad \text{(Eq. 11)}$$

n = 2: $$\frac{[Alkyl]_0{}^2 - [Alkyl]^2}{2 * ([Alkyl][Alkyl]_0)^2} = k_{eff} * t \quad \text{(Eq. 12)}$$

General remarks:

In one experiment two reaction solutions were prepared. The reactions were performed in a consecutive order to maintain the same reaction and sampling conditions. For each reaction 10 GC samples were prepared. To achieve a constant reaction temperature a slurry of melting m-xylene (m.p. = -48°C) was prepared before the experiment.

Before the experiment three stock solutions were prepared:

Sol.A: (3-Iodobutyl)benzene (132.9 mg, 0.51 mmol) and naphthalene (41.9 mg, 0.33 mmol) as an internal standard were diluted to 5.0 mL THF solution (c = 0.102 M).

Sol.B: [Fe(Bopa-Ph)Cl$(THF)_2$] (21.6 mg, 31.1 μmol) were dissolved in 5.0 mL THF (c = 6.2 mM).

Sol.C: 0.54 mL of PhMgCl in THF (1.85 M) were diluted to 4.0 mL THF solution (c = 0.25 M).

Inside the glove box screw vials with a stirring bar were filled with 1.0 mL of **Sol.A**, and then 1.0 mL of **Sol.B** was added. The vials were closed with a rubber septum. 0.5 mL of **Sol.C** was put in 1.0 mL insulin syringes (the tip of the needle was put in a rubber stopper to minimize the exposure to air). The vials were taken out of the glove box and attached to the Schlenk line by piercing a needle through the septum. The following procedure was done consecutively with every reaction vial: The vial was put in the previously prepared m-xylene slurry, and stirred for about 5 minutes (to be sure that the temperature is constant). Then the rubber septum was removed from the vial (while maintaining the nitrogen flow). **Sol.C** was added at once. An aliquot of 100 μL was taken every 45 seconds and immediately pipetted in a GC vial containing 50 μL acetonitrile. The GC vials were then filled with diethyl ether and analyzed by GC (a FI-detector was used for quantification).

Graphs show the 3 scenarios described above in Eq. 10 - 12.

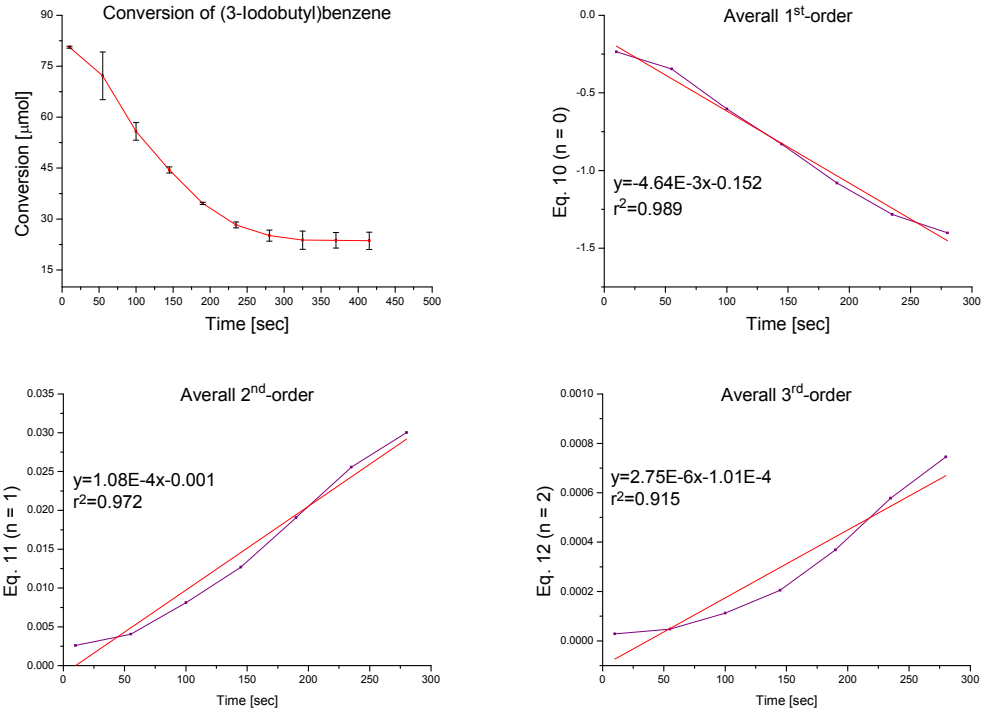

Figure S16. Results of the integrated rate law method. Graph A shows the conversion of (3-iodobutyl)benzene over the time. Graphs B – C show the results of Eq. 10 – 12. The last 3 data points at (325, 370, and 415 seconds) were not included in the calculations.

1.9. Determination of the Resting State:

Before the experiment two stock solutions were prepared:

Sol.A: (3-Iodobutyl)benzene (388.1 mg, 1.49 mmol) and [Fe(Bopa-Ph)Cl_2] (44.0 mg, 75.2 µmol) were diluted to 5.0 mL THF solution.

Sol.B: 0.97 mL of PhMgCl in THF (1.85 M) was diluted to 5.0 mL THF solution.

Sol.A and **Sol.B** were found to be too concentrated; therefore they were diluted 1:10.

Inside the glove box 28 mL were put in a 50 mL round bottom flask and cooled to -40°C. Then the UV-Probe was tipped in. After 15 minutes 1.0 mL **Sol.A** was added, and the measurement was started. Then **Sol.B** was added, and a UV/Vis spectrum was measured every 30 seconds for 10 minutes. The reaction was repeated 2 times.

If the reaction was monitored at room temperature, the immediate spectrum of the reaction mixture was identical to that observed after 10 min at -40°C. No intermediate spectrum was observed.

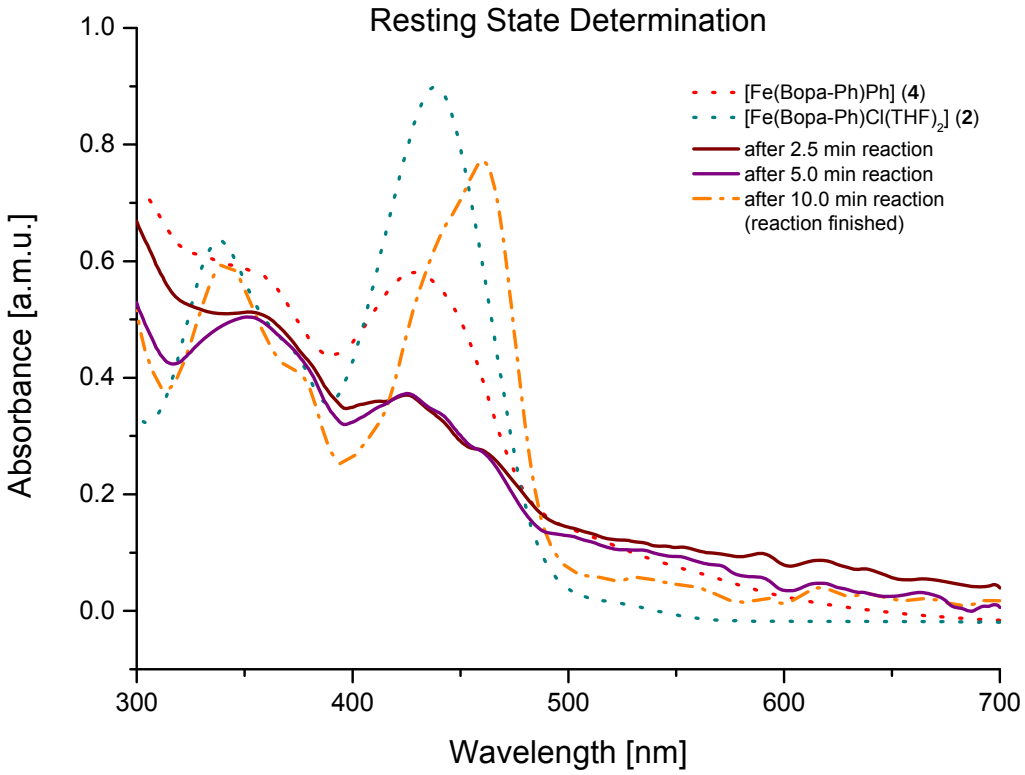

Figure S17. Absorption spectra of reaction mixture during a catalytic coupling of (3-iodobutyl)benzene with PhMgCl using **1** as catalyst.

2. Crystal Structures

2.1. [Fe(Bopa-Ph)Cl_2] (1): CCDC number 1004323

Empirical formula	$C_{30}H_{24}Cl_2FeN_3O_2$
Formula weight	585.27
Temperature	140(2) K
Wavelength	0.71073 Å
Crystal system	Orthorhombic
Space group	$P2_12_12_1$
Unit cell dimensions	a = 9.829(4) Å α= 90°.
	b = 13.481(3) Å β= 90°.
	c = 19.904(7) Å γ = 90°.
Volume	2637.4(15) $Å^3$
Z	4
Density (calculated)	1.474 Mg/m^3
Absorption coefficient	0.808 mm^{-1}
F(000)	1204
Crystal size	0.38 x 0.26 x 0.19 mm^3
Theta range for data collection	2.31 to 25.53°.
Index ranges	$-11 \le h \le 11$, $-16 \le k \le 16$, $-22 \le l \le 22$
Reflections collected	4714
Independent reflections	4714 [R_{int} = 0.0000]
Completeness to theta = 25.00°	96.1 %
Absorption correction	None
Refinement method	Full-matrix least-squares on F^2
Data / restraints / parameters	4714 / 0 / 344
Goodness-of-fit on F^2	1.038
Final R indices [I>2σ(I)]	R1 = 0.0670, wR2 = 0.1592
R indices (all data)	R1 = 0.0880, wR2 = 0.1747
Absolute structure parameter	0.04(3)
Largest diff. peak and hole	0.911 and -0.975 e.$Å^{-3}$

2.2. [Fe(Bopa-Ph)Cl$(THF)_2$] (2): CCDC number 1004324

Empirical formula	$C_{38}H_{40}ClFeN_3O_4$
Formula weight	694.03
Temperature	293(2) K
Wavelength	1.54178 Å
Crystal system	Tetragonal
Space group	$P4_32_12$
Unit cell dimensions	a = 16.2274(2) Å α= 90°.
	b = 16.2274(2) Å β= 90°.
	c = 13.1725(3) Å γ = 90°.
Volume	3468.71(11) $Å^3$
Z	4
Density (calculated)	1.329 Mg/m^3
Absorption coefficient	4.545 mm^{-1}

F(000)	1456
Crystal size	0.28 x 0.25 x 0.19 mm^3
Theta range for data collection	3.85 to 73.56°.
Index ranges	$-20 \leq h \leq 20$, $-16 \leq k \leq 20$, $-15 \leq l \leq 16$
Reflections collected	24779
Independent reflections	3480 [R_{int} = 0.0408]
Completeness to theta = 73.56°	99.7 %
Absorption correction	Semi-empirical from equivalents
Max. and min. transmission	1.00000 and 0.42332
Refinement method	Full-matrix least-squares on F^2
Data / restraints / parameters	3480 / 81 / 242
Goodness-of-fit on F2	1.046
Final R indices [I>2σ(I)]	R1 = 0.0306, wR2 = 0.0804
R indices (all data)	R1 = 0.0373, wR2 = 0.0840
Absolute structure parameter	0.000(4)
Largest diff. peak and hole	0.229 and -0.295 e.$Å^{-3}$

2.3. [Fe(Bopa-Ph)*o*Tol] (5): CCDC number 1004325

Empirical formula	$C_{41}H_{39}FeN_3O_4$
Formula weight	693.60
Temperature	140(2) K
Wavelength	0.71073 Å
Crystal system	Orthorhombic
Space group	$P2_12_12_1$
Unit cell dimensions	a = 10.295(3) Å α= 90°.
	b = 18.192(4) Å β= 90°.
	c = 20.799(5) Å γ = 90°.
Volume	3895.4(17) $Å^3$
Z	4
Density (calculated)	1.183 Mg/m^3
Absorption coefficient	0.429 mm^{-1}
F(000)	1456
Crystal size	0.41 x 0.36 x 0.21 mm^3
Theta range for data collection	2.78 to 27.68°.
Index ranges	$-13 \leq h \leq 13$, $-23 \leq k \leq 23$, $-27 \leq l \leq 27$
Reflections collected	9032
Independent reflections	9032 [R_{int} = 0.0000]
Completeness to theta = 27.68°	99.3 %
Absorption correction	None
Refinement method	Full-matrix least-squares on F^2
Data / restraints / parameters	9032 / 0 / 445
Goodness-of-fit on F^2	0.941
Final R indices [I>2σ(I)]	R1 = 0.0721, wR2 = 0.1602
R indices (all data)	R1 = 0.1084, wR2 = 0.1797
Absolute structure parameter	0.03(2)
Extinction coefficient	0.030(2)
Largest diff. peak and hole	0.496 and -0.641 e.$Å^{-3}$

3. Computational Details

Geometries of all species were optimized in the gas-phase at the unrestricted M06[16,178]/def2-SVP level using the "Ultrafine" grid in Gaussian09.[19] The relative energetics of the various spin states of the Fe complexes **4**, **13**, **14**, **15** were confirmed from computations using both the M06 and OPBE[10,20] functionals (Table S3). The later functional feature OPTZ exchange, which assists in the accurate reproduction of energies of inorganic complexes with different spin states.[21-23] The M06/def2-SVP geometries of relevant compounds were then recomputed as single point energies using a density-dependent dispersion correction[12-15] appended to the PBE0[10,11] functional (PBE0-dDsC) with the triple-ζ slater-type orbital TZ2P basis set in ADF.[24,25] Solvation corrections (in THF) employed the continuum solvent model for realistic solvents[18] (COSMO-RS), as implemented in ADF. The minimum energy crossing point of **15** was located using the "MECP Location Program" of Harvey.[26] The supplemental file Fe_Coupling_CartesianCoords contains the computed Cartesian coordinates of all of the molecules reported in this study.

Table S3. Optimized geometries of relevant complexes in different spin states.

Species	M06/def2-SVP Electronic Energy (hartree)	M06 Relative Energy (kcal/mol)	OPBE/def2-SVP Electronic Energy (hartree)	OPBE Relative Energy (kcal/mol)
4 – Singlet	-2621.383964	37.54	-2622.136822	19.30
4 – Triplet	-2621.419003	15.55	-2622.155719	7.44
4 – Quintet	-2621.443786	0.00	-2622.167577	0.00
13 – Doublet	-3081.502578	26.85	-3082.217543	12.14
13 – Quartet	-3081.532439	8.11	-3082.234075	1.77
13 – Sextet	-3081.545366	0.00	-3082.236894	0.00
14 – Singlet	Dissociates	NA	Dissociates	NA
14 – Triplet	Dissociates	NA	-3200.534437	11.32
14 – Quintet	-3199.824253	0.00	-3200.552481	0.00
15 – Doublet	-2739.741886	13.67	-2740.514266	1.16
15 – Quartet	-2739.753196	6.57	-2740.512905	2.01

15 - Sextet	-2739.763670	0.00	-2740.516107	0.00

Table S4. Electronic energies (hartree), free energy corrections (hartree) and solvation corrections (in kcal/mol) for relevant compounds.

Compound	M06/def2-SVP Electronic Energy	M06/def2-SVP Free Energy Correction	PBE0-dDsC/TZ2P Electronic Energy	PBE0-dDSC COMSO-RS Solvation Energy
4+iPr•	-2739.742173	0.501147	-19.806264	-20.776
$TS_{4,15}$	-2739.737126	0.505133	-19.801997	-19.701
15_{Sextet}	-2739.763670	0.508481	-19.824147	-18.343
15_{MECP}	-2739.746587	0.508551	-19.807272	-18.080
$15_{Quartet}$	-2739.753196	0.511789	-19.818664	-17.771
$15'_{Quartet}$	-2739.760219	0.510125	-19.830210	-19.178
$TS_{15,16}$	-2739.739211	0.512545	-19.804448	-18.294
16	-2739.802550	0.514368	-19.848242	-18.392
13+iPr•	-3199.831366	0.503913	-19.972166	-21.329
$TS_{13,14}$	-3199.824052	0.511594	-19.963281	-21.128
14	-3199.824253	0.512781	-19.964321	-20.899
$TS_{14,2X}$	-3199.819698	0.513414	-19.958890	-21.325
2X	-3199.938674	0.512279	-20.082926	-21.232

Table S5. Contributions to reaction free energies (in kcal/mol).

Reaction	M06/def2-SVP Electronic Energy	M06/def2-SVP Free Energy Correction	PBE0-dDsC/TZ2P Electronic Energy	PBE0-dDSC COMSO-RS Solvation Energy
Bimetallic Oxidative Addition				
4+iPr• → **$TS_{4,15}$**	3.17	2.50	2.68	1.08
$TS_{4,15}$ → **15_{Sextet}**	-16.66	2.10	-13.90	1.36
15_{Sextet} → **15_{MECP}**	10.72	0.04	10.59	0.26

15_{MECP} → $15_{Quartet}$	-4.15	2.03	-7.15	0.31
$15_{Quartet}$ → $15'_{Quartet}$	-4.41	-1.04	-7.25	-1.41
$15'_{Quartet}$ → $TS_{15,16}$	13.18	1.52	16.17	0.88
$TS_{15,16}$ → $16_{Quartet}$	-39.75	1.14	-27.48	-0.10
Escape Rebound				
13+iPr• → **$TS_{13,14}$**	4.59	4.82	5.58	0.20
$TS_{13,14}$ → 14	-0.13	0.74	-0.65	0.23
14 → $TS_{14,2X}$	2.86	0.40	3.41	-0.43
$TS_{14,2X}$ → 2X	-74.66	-0.71	-77.83	0.09

4. Appendix

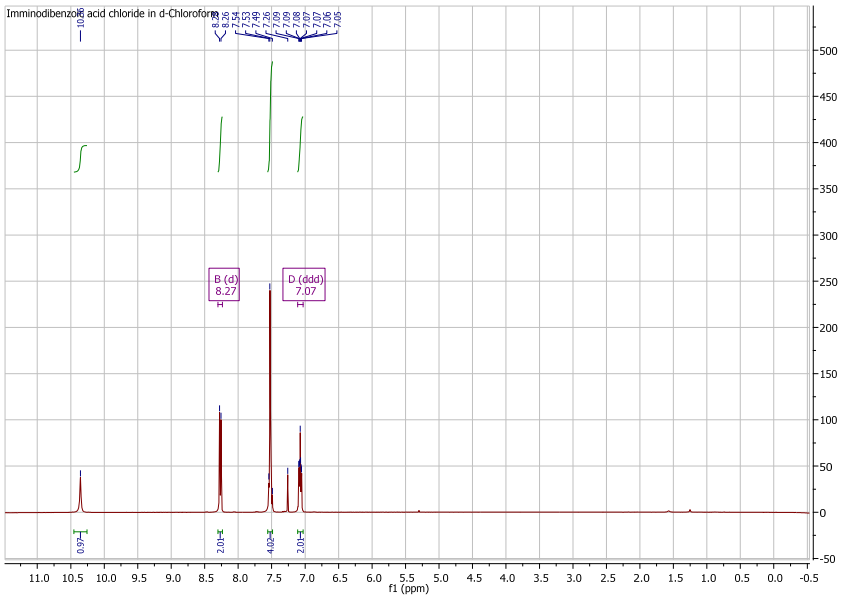

Figure S18. ^{1}H-NMR spectrum of imminodibenzoic acid chloride

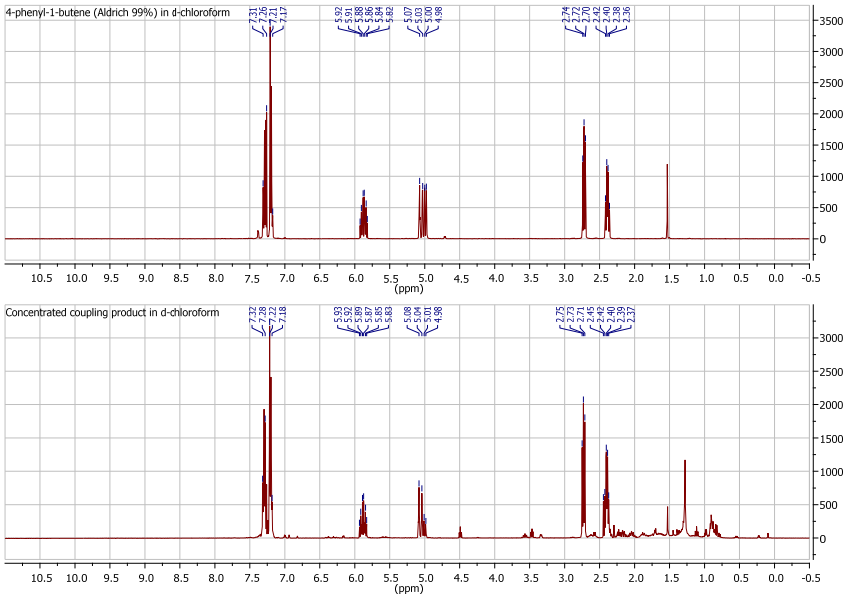

Figure S19. Phenylbutene ring opening radical probe.

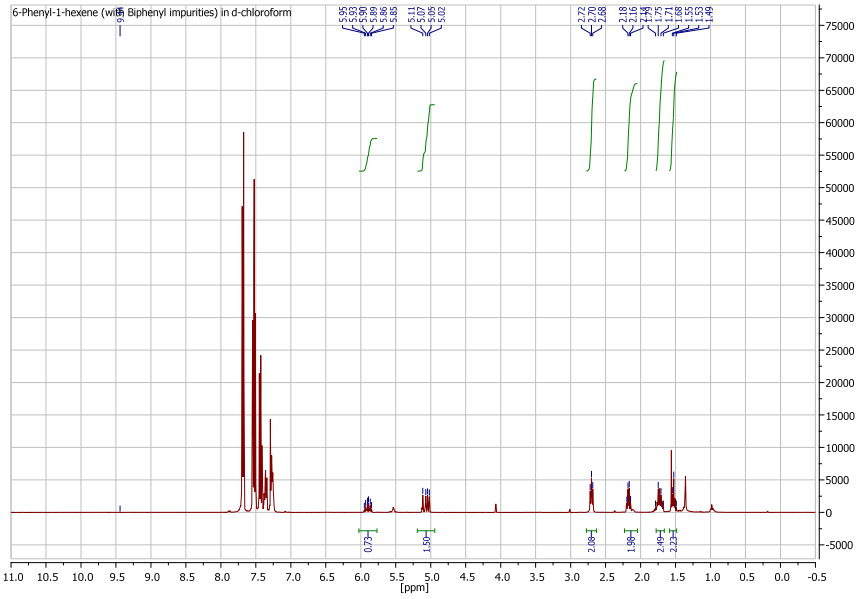

Figure S20. ^{1}H-NMR of 6-Phenyl-1-hexene (with biphenyl impurities).

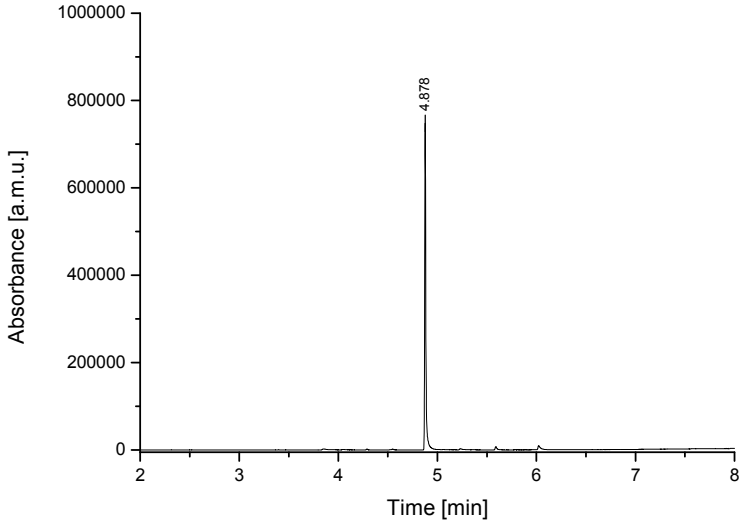

Figure S21. GC spectrum of 1,3-diphenylpropane directly synthesized as a reference.

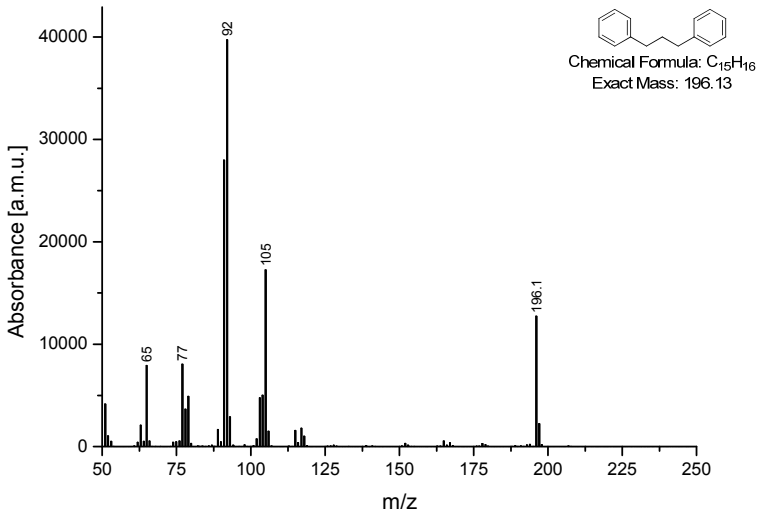

Figure S22. Averaged MS-spectrum between 4.87-4.89 min retention time (MS spectrum corresponding to the GC spectrum in Figure S21).

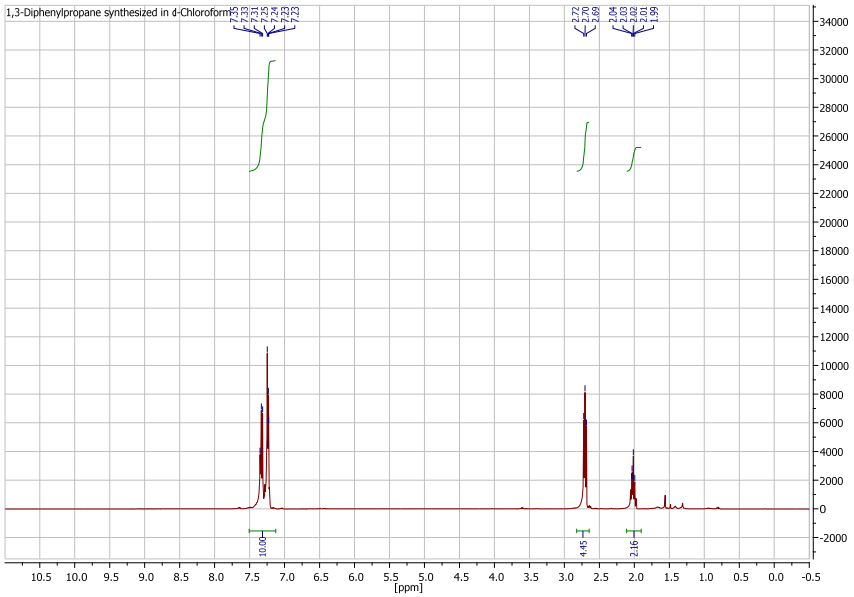

Figure S23. ^{1}H-NMR spectrum of synthesized 1,3-diphenylpropane (corresponding to the GC spectrum in Figure S21).

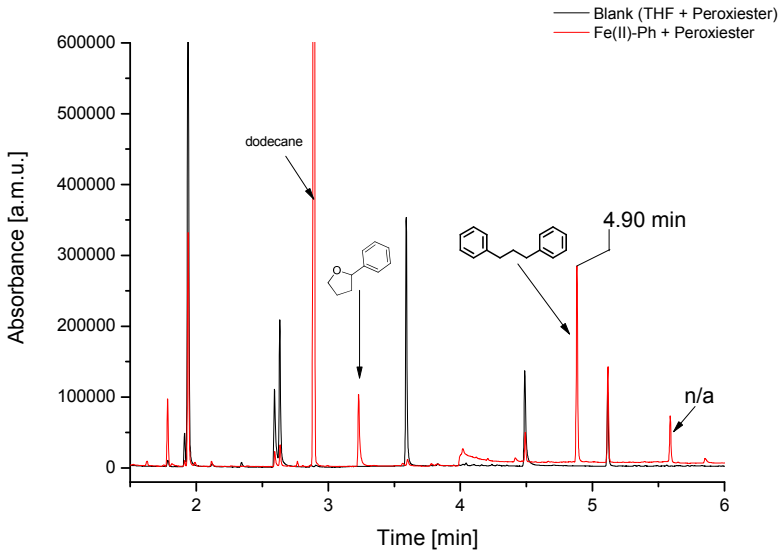

Figure S25. Superposition of the reaction of [Fe(Bopa-Ph)Ph] with *tert*-butyl-4-phenylbutaneperoxate and its blank reaction (*tert*-butyl-4-phenylbutaneperoxate in THF).

5. References

(1) Paul, A.; Ladame, S. *Organic Letters* **2009**, *11*, 4894.

(2) McKennon, M. J.; Meyers, A. I.; Drauz, K.; Schwarm, M. *The Journal of Organic Chemistry* **1993**, *58*, 3568.

(3) Csok, Z.; Vechorkin, O.; Harkins, S. B.; Scopelliti, R.; Hu, X. L. *Journal of the American Chemical Society* **2008**, *130*, 8156.

(4) Inagaki, T.; Phong, L. T.; Furuta, A.; Ito, J.-i.; Nishiyama, H. *Chemistry – A European Journal* **2010**, *16*, 3090.

(5) Crosignani, S.; Nadal, B.; Li, Z.; Linclau, B. *Chemical Communications* **2003**, 260.

(6) Rueda-Becerril, M.; Chatalova Sazepin, C.; Leung, J. C. T.; Okbinoglu, T.; Kennepohl, P.; Paquin, J.-F.; Sammis, G. M. *Journal of the American Chemical Society* **2012**, *134*, 4026.

(7) Love, B. E.; Jones, E. G. *The Journal of Organic Chemistry* **1999**, *64*, 3755.

(8) Lu, S.-F.; Du, D.-M.; Zhang, S.-W.; Xu, J. *Tetrahedron: Asymmetry* **2004**, *15*, 3433.

(9) Gamage, S. A.; Smith, R. A. J. *Tetrahedron* **1990**, *46*, 2111.

(10) Perdew, J. P.; Burke, K.; Ernzerhof, M. *Phys. Rev. Lett.* **1996**, *77*, 3865.

(11) Adamo, C.; Barone, V. *J. Chem. Phys.* **1999**, *110*, 6158.

(12) Steinmann, S. N.; Corminboeuf, C. *J. Chem. Theory Comput.* **2010**, *6*, 1990.

(13) Steinmann, S. N.; Corminboeuf, C. *Chimia* **2011**, *65*, 240.

(14) Steinmann, S. N.; Corminboeuf, C. *J. Chem. Phys.* **2011**, *134*, 044117.

(15) Steinmann, S. N.; Corminboeuf, C. *J. Chem. Theory Comput.* **2011**, 3567.

(16) Zhao, Y.; Truhlar, D. G. *Theor. Chem. Acc.* **2008**, *120*, 215.

(17) Zhao, Y.; Truhlar, D. G. *Acc. Chem. Res.* **2008**, *41*, 157.

(18) Klamt, A. *WIREs Comp. Mol. Sci.* **2011**, *1*, 699.

(19) Frisch, M. J.; Trucks, G. W.; Schlegel, H. B.; Scuseria, G. E.; Robb, M. A.; Cheeseman, J. R.; Scalmani, G.; Barone, V.; Mennucci, B.; Petersson, G. A.; Nakatsuji, H.; Caricato, M.; Li, X.; Hratchian, H. P.; Izmaylov, A. F.; Bloino, J.; Zheng, G.; Sonnenberg, J. L.; Hada, M.; Ehara, M.; Toyota, K.; Fukuda, R.; Hasegawa, J.; Ishida, M.; Nakajima, T.; Honda, Y.; Kitao, O.; Nakai, H.; Vreven, T.; Montgomery, J., J. A.; Peralta, J. E.; Ogliaro, F.; Bearpark, M.; Heyd, J. J.; Brothers, E.; Kudin, K. N.; Staroverov, V. N.; Kobayashi, R.; Normand, J.; Raghavachari, K.; Rendell, A.; Burant, J. C.; Iyengar, S. S.; Tomasi, J.; Cossi, M.; Rega, N.; Millam, M. J.; Klene, M.; Knox, J. E.; Cross, J. B.; Bakken, V.; Adamo, C.; Jaramillo, J.; Gomperts, R.; Stratmann, R. E.; Yazyev, O.; Austin, A. J.; Cammi, R.; Pomelli, C.; Ochterski, J. W.; Martin, R. L.; Morokuma, K.; Zakrzewski, V. G.; Voth, G. A.; Salvador, P.; Dannenberg, J. J.; Dapprich, S.; Daniels, A. D.; Farkas, O.; Foresman, J. B.; Ortiz, J. V.; Cioslowski, J.; Fox, D. J. Gaussian 09, Revision D.01; Gaussian, Inc.: Wallingford, CT, 2009.

(20) Handy, N. C.; Cohen, A. J. *Mol. Phys.* **2001**, *99*, 403.

(21) Conradie, J.; Ghosh, A. *J. Phys. Chem. B* **2007**, *111*, 12621.

(22) Rotzinger, F. P. *J. Chem. Theory Comput.* **2009**, *5*, 1061.

(23) Curchod, B. F. E.; Rotzinger, F. P. *Inorg. Chem.* **2011**, *50*, 8728.

(24) te Velde, G.; Bickelhaupt, F. M.; van Gisbergen, S. J. A.; Fonseca Guerra, C.; Baerends, E. J.; Snijders, J. G.; Ziegler, T. *J. Comput. Chem.* **2001**, *22*, 931.

(25) Fonseca Guerra, C.; Snijders, J. G.; te Velde, G.; Baerends, E. J. *Theor. Chem. Acc.* **1998**, *99*, 391.

(26) Harvey, J. N.; Aschi, M.; Schwarz, H.; Koch, W. *Theor. Chem. Acc.* **1998**, *99*, 95.